nature nanotechnology

SUPPLEMENTARY INFORMATION

DOI: 10.1038/NNANO.2015.309

Tailoring high-temperature radiation and the resurrection of the incandescent source

Ognjen Ilic, Peter Bermel, Gang Chen, John D. Joannopoulos, Ivan Celanovic, and Marin Soljačić

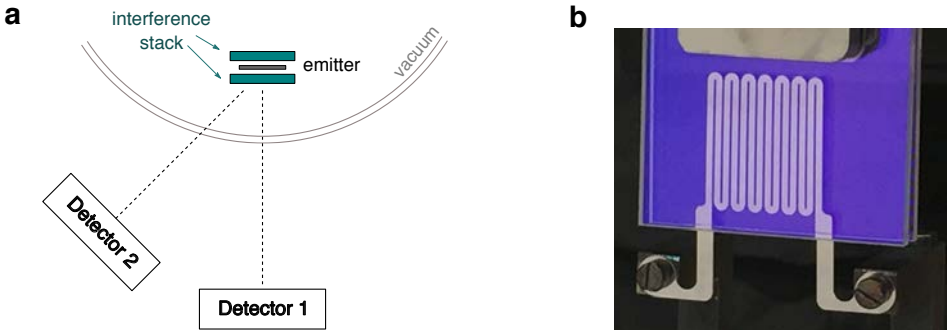

Supplementary Fig. 1 | Sketch of the experimental setup. (a) Two detectors measure the emitted spectra at 0° and 45° angles with respect to the surface of the emitter. They are calibrated to correct for any nonlinearity in the measured signal. The air in the setup is evacuated (P$\sim 10^{-6}$ torr) and argon is added (P$\sim 10^{-4}$ torr). (b) Tungsten emitter and surrounding interference stacks (on fused silica substrate) in the experimental setup.

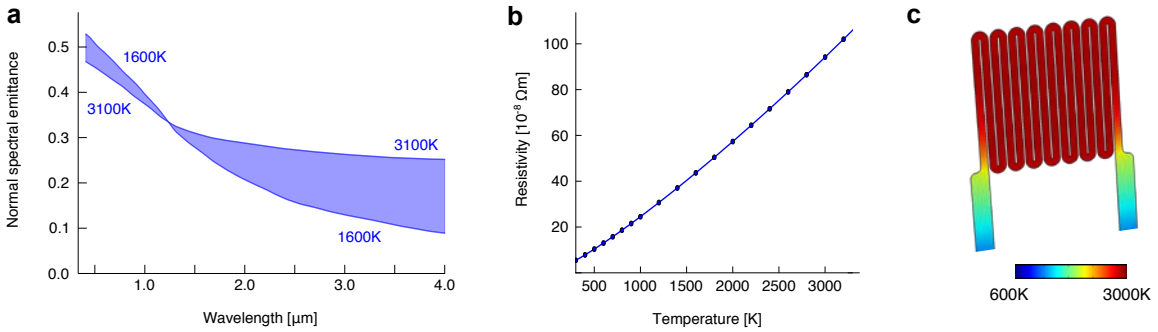

Supplementary Fig. 2 | Thermal emitter properites. (a) General trend for the high temperature normal spectral emittance of polished tungsten[31], with a caveat that high temperature optical properties of refractory metals strongly depend on material purity and sample preparation. The shaded region covers the temperature range of 1600K-3100K. (b) Tungsten resistivity as a function of temperature[34], used to estimate the temperature of the heated emitter. (c) Temperature distribution in a heated emitter (obtained by finite-element analysis, see Methods).

DOI: 10.1038/NNANO.2015.309

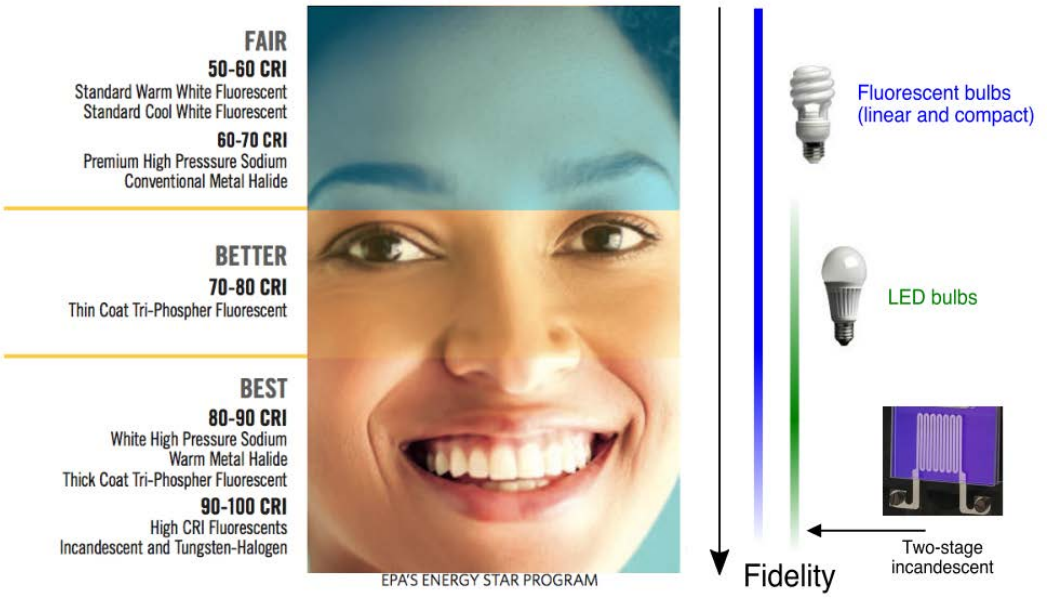

Supplementary Fig. 3 | Colour rendering index (CRI) comparison. Image (includes text) to the left of the fidelity arrow obtained from EnergyStar.gov. The rest of the figure is superimposed by the authors, using values from the main text of the manuscript (CFL and LED bulb pictures obtained from Energy.gov). For the CRI estimation of our device we use the hemispherical emittance values (corresponding to capturing the light output at every angle, for example in a reflector enclosure).

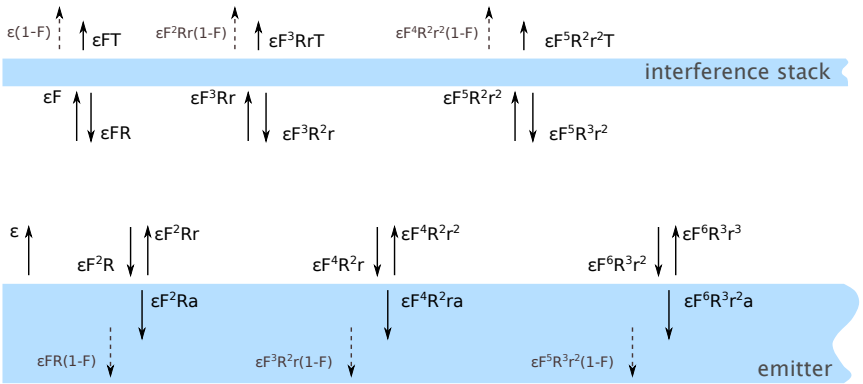

Supplementary Fig. 4 | Ray-tracing analysis for effective thermal emission. Analysis is performed (left to right) for the thermal emitter (bottom) surrounded by a reflecting interference stack (top). Stack transmissivity and reflectivity are denoted by $T(\lambda)$ and $R(\lambda)$, respectively. Emitter emissivity is denoted by $\epsilon(\lambda)$, absorptivity by $a(\lambda) = \epsilon(\lambda)$, and reflectivity by $r(\lambda) = 1\epsilon(\lambda)$. Dashed arrows denote escaped rays that are not captured by either the emitter or the filtering structure.

Derivation of the effective emissivity for thermal radiation. Our model assumes a thermal emitter of emissivity $\epsilon(\lambda, T)$, surrounded by an interference structure of reflectivity $R(\lambda)$ and transmissivity $T(\lambda)$. These labels refer to hemispherical quantities. E.g. for emissivity, if θ denotes the

polar angle relative to the emitter surface, the spectral hemispherical emissivity can be expressed as:

$$\epsilon(\lambda) = \frac{\int_0^{\pi/2} \epsilon(\lambda,\theta)\sin(\theta)\cos(\theta)d\theta}{\int_0^{\pi/2} \sin(\theta)\cos(\theta)d\theta} \tag{S1}$$

where $\epsilon(\lambda,\theta)$ is the directional spectral emissivity. We assume the emissivity does not depend on the azimuthal angle (ϕ).

The emitter-interference structure geometry is characterized by a view-factor F, which equals the proportion of diffuse energy leaving the emitter that is directly intercepted by the surface of the filtering structure. To obtain the effective emissivity of the system, we consider multiple ray reflections in the cavity formed by the surrounding filtering structure (see Supplementary Fig. 4). With this in mind, the expressions for the transmitted rays (P_T), the rays that escape the cavity (P_{EF}), and the back-reflected rays that escape the thermal emitter (P_{EE}) are given by:

$$\begin{aligned}
P_T/P_0 &= \epsilon FT + \epsilon F^3 RrT + \epsilon F^5 R^2 r^2 T + \ldots \\
&= \epsilon FT\left[1 + F^2 Rr + F^4 R^2 r^2 + \ldots\right] \\
&= \epsilon \frac{FT}{1 - F^2 R(1-\epsilon)} \\
P_{EF}/P_0 &= \epsilon(1-F) + \epsilon(1-F)F^2 Rr + \epsilon(1-F)F^4 R^2 r^2 + \ldots \\
&= \epsilon(1-F)\left[1 + F^2 Rr + F^4 R^2 r^2 + \ldots\right] \\
&= \epsilon \frac{1-F}{1 - F^2 R(1-\epsilon)} \\
P_{EE}/P_0 &= \epsilon FR(1-F) + \epsilon F^3 R^2 r(1-F) + \epsilon F^5 R^3 r^2 (1-F) + \ldots \\
&= \epsilon(1-F)FR\left[1 + F^2 Rr + F^4 R^2 r + \ldots\right] \\
&= \epsilon \frac{(1-F)FR}{1 - F^2 R(1-\epsilon)}
\end{aligned} \tag{S2}$$

Combining the terms above, we obtain the effective emissivity as:

$$\epsilon_{eff} = \epsilon\left[\frac{FT}{1 - F^2 R(1-\epsilon)} + \frac{(1-F)(1+FR)}{1 - F^2 R(1-\epsilon)}\right] \tag{S3}$$

which reproduces equation (1) of the main text. The amount of power reabsorbed by the emitter (P_r) can be calculated by summing up the contributions of all back-reflected rays:

$$\begin{aligned}
P_r &= P_0 \epsilon\left[F^2 Ra + F^2 RrF^2 Ra + F^2 RrF^2 RrF^2 Ra + \ldots\right] \\
P_r &= P_0 \epsilon F^2 Ra \sum_{n=0}^{\infty}\left[F^2 Rr\right]^n \\
P_r &= P_0 \frac{\epsilon^2 F^2 R}{1 - F^2 R(1-\epsilon)}
\end{aligned} \tag{S4}$$

where the absorptivity of the emitter is given by Kirchoff's law $a(\lambda,T) = \epsilon(\lambda,T)$, and its reflectivity is equal to $r(\lambda,T) = 1 - a(\lambda,T)$ (no transmission). Here P_0 is the power originally emitted by the plain emitter at the same temperature. The emissivity above takes into account emission into all angles (hemispherical emissivity).

DOI: 10.1038/NNANO.2015.309

Analysis of diffuse versus specular elements. In the preceding section of the supplement, we approximated active surfaces (emitter and interference structure) as diffuse emitters as well as diffuse reflectors. This means that the optical properties of such structures are independent of direction. While the assumption of diffuse emission is often acceptable[41], many optical elements may not be always adequately described as diffuse reflectors. In our case, both the polished metal emitter, as well as the interference multilayer stack may exhibit specular reflection peaks in the visible as well as the infra-red. With this in mind, we extend our analysis to include specular (e.g. mirror-like) reflections. As it turns out, in the geometry of our system, this distinction is not especially relevant, particularly for the integrated system quantities (such as the luminous efficiency, total absorbed and emitted power, etc.).

In contrast to the definition of a diffuse view factor, a specular view factor takes into account light intercepted by the receiving element via direct travel or any number of intermediate specular reflections. For two parallel directly opposed rectangles (labelled 1 and 2), of the same width and length, the specular view factor can be expressed as[42]:

$$F^s_{12} = F^s_{21} = K(1) + \sum_{n=1}^{\infty} R^n K(2n+1) \tag{S5}$$

$$\frac{F^s_{11}}{r^s_2} = \frac{F^s_{22}}{r^s_1} = K(2) + \sum_{n=1}^{\infty} R^n K(2n+2) \tag{S6}$$

Here, $R = r^s_1 r^s_2$ is the product of specular reflection coefficients of the two rectangular plates, and

$$K(m) = \frac{2m^2}{\pi X^2 Z}\left[K_1(m) + K_2(m) + K_3(m)\right] \tag{S7}$$

where

$$K_1(m) = \ln\left[\frac{(1+(X/m)^2)(1+(XZ/m)^2}{1+(X/m)^2+(XZ/m)^2}\right]^{1/2}$$

$$K_2(m) = \frac{XZ}{m}\left[\sqrt{1+(X/m)^2}\tan^{-1}\frac{XZ/m}{\sqrt{1+(X/m)^2}} - \tan^{-1}\frac{XZ}{m}\right]$$

$$K_3(m) = \frac{X}{m}\left[\sqrt{1+(XZ/m)^2}\tan^{-1}\frac{X/m}{\sqrt{1+(XZ/m)^2}} - \tan^{-1}\frac{X}{m}\right]$$

with $X = a/D$, $Z = b/a$, where a, b are the lengths of sides of the rectangles, and D is the distance between them. We observe that the specular view factor, by definition, includes the multiple reflections that are the basis of equations (S2)-(S4). In addition, we note that the view factor depends on the reflectivity properties of the surface, which was not the case for the diffuse view factor.

Our system consists of an emitter and a surrounding interference structure (labelled 1 and 2) and the four surrounding sides (together labelled 3). Using the sum rule for the specular view factors in an enclosure, we write:

$$F^s_{13} = 1 - (1-R^s)F^s_{12} - (1-r^s)F^s_{11} \tag{S8}$$

where F^s_{13} is the specular view factor from the thermal emitter to the surrounding sides, and F^s_{13} is the specular view factor from the emitter to the filtering structure. Finally, the effective emissivity can be expressed as $\epsilon_{eff} = \epsilon\left[F^s_{12}T + F^s_{13}\right]$. For specular reflections, we found the difference in the integrated

system quantities relative to the purely diffuse case to be rather small: for luminous efficiency, the difference is under 5%; similar values apply to flux quantities, such as the total absorbed or total radiated power. The fact that heat flux calculations in our system are not very sensitive to the diffuse versus specular distinction is not too surprising. In fact, for most practical enclosures it suffices to calculate heat fluxes assuming purely diffuse reflectors, notable exceptions being active elements at the ends of long and narrow channels, and configurations with collimated irradiation[41]. Moreover, we recall the desired properties of an optimal interference structure - it has similar spectral properties for a broad range of angles. Hence, the ideal design has a directional reflectance that is close to the averaged, hemispherical value.

Interference structure specifications. The fabricated interference structure consists of 90 layers of alternating high (Ta_2O_5) and low (SiO_2) refractive index films of varying thicknesses. Starting from an optimal chirped quarterwave stack design (green, Fig. 1), the structure is further optimized as described in the Methods section. The optical profile of the fabricated interference structure (refractive index vs. the structure thickness) is shown in Supplementary Fig. 5 (for $\lambda = 610$nm; refractive indices necessarily have dispersion). For clarity, we also present the interference structure specifications in a tabular form, both for the fabricated structure (shown in blue in Fig. 2) as well as for the structure that optimizes luminous efficiency (shown in red in Fig. 1; here $n_{Al_2O_3} = 1.68$, $n_{TiO_2} = 2.35$).

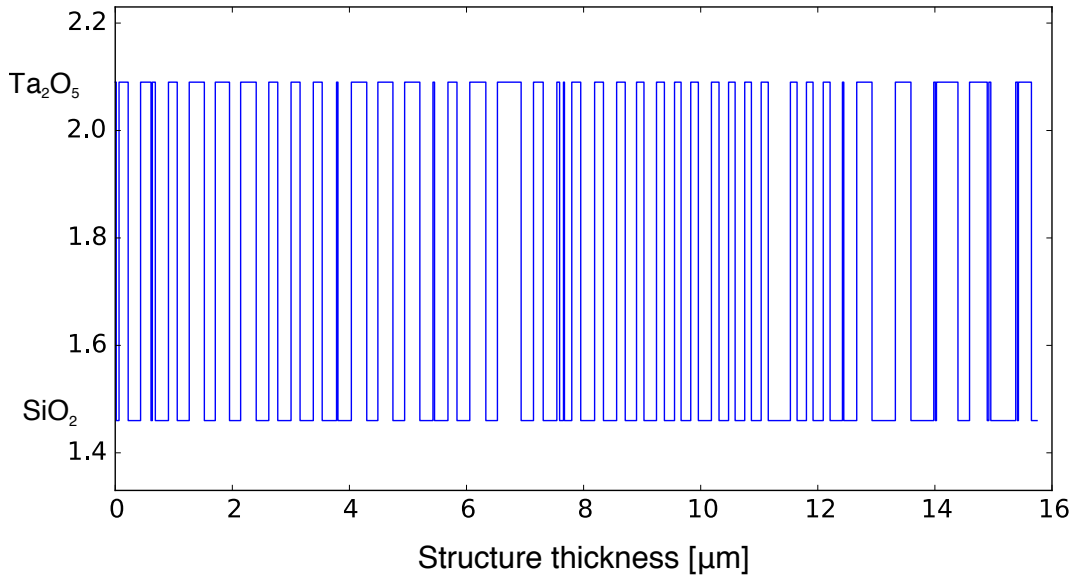

Supplementary Fig. 5 | Refractive index profile of the 90-layer fabricated interference. structure.

References (Supplementary Materials)

41. Modest, M. Radiative Heat Transfer (Academic Press, ed. 3, 2013).

42. "Thermal design handbook - Part 1: View factors", European Cooperation for Space Standardization (ECSS) Handbooks and Technical Memoranda (ECSS-E-HB-31-01 Part 1A, 2011).

DOI: 10.1038/NNANO.2015.309

#	D [nm]	Material	#	D [nm]	Material	#	D [nm]	Material
1	18	Ta2O5	31	27	Ta2O5	61	112	Ta2O5
2	47	SiO2	32	229	SiO2	62	164	SiO2
3	156	Ta2O5	33	154	Ta2O5	63	114	Ta2O5
4	212	SiO2	34	219	SiO2	64	167	SiO2
5	178	Ta2O5	35	274	Ta2O5	65	121	Ta2O5
6	23	SiO2	36	198	SiO2	66	378	SiO2
7	51	Ta2O5	37	405	Ta2O5	67	114	Ta2O5
8	224	SiO2	38	211	SiO2	68	160	SiO2
9	150	Ta2O5	39	166	Ta2O5	69	113	Ta2O5
10	205	SiO2	40	233	SiO2	70	174	SiO2
11	258	Ta2O5	41	47	Ta2O5	71	117	Ta2O5
12	187	SiO2	42	66	SiO2	72	211	SiO2
13	243	Ta2O5	43	17	Ta2O5	73	23	Ta2O5
14	190	SiO2	44	125	SiO2	74	221	SiO2
15	266	Ta2O5	45	153	Ta2O5	75	261	Ta2O5
16	215	SiO2	46	237	SiO2	76	399	SiO2
17	153	Ta2O5	47	151	Ta2O5	77	266	Ta2O5
18	227	SiO2	48	225	SiO2	78	390	SiO2
19	154	Ta2O5	49	147	Ta2O5	79	28	Ta2O5
20	226	SiO2	50	193	SiO2	80	18	SiO2
21	152	Ta2O5	51	127	Ta2O5	81	367	Ta2O5
22	245	SiO2	52	214	SiO2	82	198	SiO2
23	24	Ta2O5	53	135	Ta2O5	83	302	Ta2O5
24	229	SiO2	54	173	SiO2	84	28	SiO2
25	263	Ta2O5	55	112	Ta2O5	85	33	Ta2O5
26	190	SiO2	56	165	SiO2	86	426	SiO2
27	257	Ta2O5	57	130	Ta2O5	87	31	Ta2O5
28	200	SiO2	58	223	SiO2	88	15	SiO2
29	260	Ta2O5	59	130	Ta2O5	89	222	Ta2O5
30	224	SiO2	60	163	SiO2	90	96	SiO2

Supplementary Fig. 6 | Specifications for the 90-layer fabricated interference structure.

#	D [nm]	Material	#	D [nm]	Material	#	D [nm]	Material	#	D [nm]	Material
1	494	TiO2	81	36	Al2O3	161	9	Al2O3	241	126	Al2O3
2	500	SiO2	82	436	SiO2	162	296	SiO2	242	138	TiO2
3	94	Al2O3	83	112	Al2O3	163	111	Al2O3	243	169	SiO2
4	490	TiO2	84	245	TiO2	164	192	TiO2	244	110	TiO2
5	118	Al2O3	85	162	SiO2	165	76	Al2O3	245	167	SiO2
6	500	SiO2	86	38	Al2O3	166	114	SiO2	246	114	TiO2
7	117	Al2O3	87	343	TiO2	167	210	TiO2	247	189	SiO2
8	500	TiO2	88	1	Ta2O5	168	21	Ta2O5	248	117	TiO2
9	115	Al2O3	89	80	Al2O3	169	50	Al2O3	249	52	Al2O3
10	500	SiO2	90	500	SiO2	170	263	SiO2	250	145	SiO2
11	123	Al2O3	91	247	TiO2	171	23	Al2O3	251	120	TiO2
12	382	TiO2	92	36	Al2O3	172	125	TiO2	252	157	SiO2
13	123	Al2O3	93	38	SiO2	173	126	Al2O3	253	121	TiO2
14	500	SiO2	94	170	Al2O3	174	123	SiO2	254	123	SiO2
15	123	Al2O3	95	259	TiO2	175	247	TiO2	255	33	Al2O3
16	383	TiO2	96	135	Al2O3	176	152	SiO2	256	116	TiO2
17	113	Al2O3	97	332	SiO2	177	103	Al2O3	257	99	SiO2
18	500	SiO2	98	56	Al2O3	178	147	TiO2	258	65	Al2O3
19	114	Al2O3	99	137	TiO2	179	94	Al2O3	259	103	TiO2
20	380	TiO2	100	96	Ta2O5	180	168	SiO2	260	152	SiO2
21	100	Al2O3	101	312	SiO2	181	105	Al2O3	261	41	Al2O3
22	500	SiO2	102	52	Al2O3	182	124	TiO2	262	99	TiO2
23	98	Al2O3	103	228	TiO2	183	69	Al2O3	263	200	SiO2
24	380	TiO2	104	173	Al2O3	184	172	SiO2	264	81	TiO2
25	112	Al2O3	105	219	SiO2	185	27	Al2O3	265	177	SiO2
26	378	SiO2	106	135	Al2O3	186	212	TiO2	266	91	TiO2
27	100	Al2O3	107	227	TiO2	187	11	Ta2O5	267	148	SiO2
28	254	TiO2	108	43	Al2O3	188	20	Al2O3	268	123	TiO2
29	73	Al2O3	109	344	SiO2	189	85	SiO2	269	90	SiO2
30	406	SiO2	110	234	TiO2	190	67	Al2O3	270	35	Al2O3
31	109	Al2O3	111	59	Al2O3	191	187	TiO2	271	120	TiO2
32	369	TiO2	112	247	SiO2	192	46	Al2O3	272	116	SiO2
33	69	Al2O3	113	31	Al2O3	193	159	SiO2	273	120	TiO2
34	500	SiO2	114	246	TiO2	194	78	Al2O3	274	161	SiO2
35	84	Al2O3	115	458	SiO2	195	121	TiO2	275	108	TiO2
36	376	TiO2	116	230	TiO2	196	56	Al2O3	276	132	SiO2
37	87	Al2O3	117	34	Ta2O5	197	242	SiO2	277	101	TiO2
38	500	SiO2	118	274	SiO2	198	31	Al2O3	278	128	SiO2
39	60	Al2O3	119	45	Al2O3	199	142	TiO2	279	95	TiO2
40	243	TiO2	120	232	TiO2	200	22	Al2O3	280	153	SiO2
41	122	Al2O3	121	335	SiO2	201	210	SiO2	281	98	TiO2
42	328	SiO2	122	54	Al2O3	202	12	Al2O3	282	105	SiO2
43	79	Al2O3	123	214	TiO2	203	189	TiO2	283	116	TiO2
44	9	Ta2O5	124	64	Al2O3	204	203	SiO2	284	90	SiO2
45	336	TiO2	125	244	SiO2	205	29	Al2O3	285	102	TiO2
46	71	Al2O3	126	104	Al2O3	206	166	TiO2	286	82	SiO2
47	500	SiO2	127	154	TiO2	207	256	SiO2	287	111	TiO2
48	41	Al2O3	128	127	Al2O3	208	148	TiO2	288	128	SiO2
49	359	TiO2	129	241	SiO2	209	220	SiO2	289	80	TiO2
50	133	Al2O3	130	36	Al2O3	210	56	Al2O3	290	198	SiO2
51	197	SiO2	131	241	TiO2	211	131	TiO2	291	6	TiO2
52	237	TiO2	132	92	Al2O3	212	203	SiO2	292	203	SiO2
53	500	SiO2	133	189	SiO2	213	164	TiO2	293	59	TiO2
54	93	Al2O3	134	78	Al2O3	214	70	Ta2O5	294	165	SiO2
55	130	Ta2O5	135	126	TiO2	215	163	SiO2	295	98	TiO2
56	243	TiO2	136	89	Al2O3	216	137	TiO2	296	89	SiO2
57	100	Al2O3	137	325	SiO2	217	104	Al2O3	297	116	TiO2
58	304	SiO2	138	54	Al2O3	218	147	SiO2	298	76	SiO2
59	111	Al2O3	139	10	Ta2O5	219	129	TiO2	299	259	TiO2
60	241	TiO2	140	219	TiO2	220	238	SiO2	300	147	SiO2
61	106	Al2O3	141	40	Al2O3	221	128	TiO2			
62	273	SiO2	142	100	SiO2	222	199	SiO2			
63	143	Al2O3	143	52	Al2O3	223	48	Al2O3			
64	259	TiO2	144	8	Ta2O5	224	131	TiO2			
65	123	Al2O3	145	218	TiO2	225	4	Al2O3			
66	461	SiO2	146	69	Al2O3	226	230	SiO2			
67	84	Al2O3	147	313	SiO2	227	128	TiO2			
68	252	TiO2	148	21	Al2O3	228	64	Al2O3			
69	152	Al2O3	149	114	TiO2	229	155	SiO2			
70	62	SiO2	150	3	Al2O3	230	130	TiO2			
71	141	Al2O3	151	362	SiO2	231	231	SiO2			
72	256	TiO2	152	69	Al2O3	232	109	TiO2			
73	75	Al2O3	153	236	TiO2	233	183	SiO2			
74	500	SiO2	154	17	Ta2O5	234	49	Al2O3			
75	92	Al2O3	155	114	Al2O3	235	137	TiO2			
76	280	TiO2	156	44	Ta2O5	236	209	SiO2			
77	143	Al2O3	157	199	TiO2	237	119	TiO2			
78	56	SiO2	158	85	Al2O3	238	210	SiO2			
79	283	TiO2	159	309	SiO2	239	119	TiO2			
80	92	Ta2O5	160	132	TiO2	240	74	SiO2			

Supplementary Fig. 7 | Specifications for the structure that optimizes luminous efficiency.